

X-RAYS FROM RADIO MILLISECOND PULSARS: COMPTONIZED THERMAL RADIATION

SLAVKO BOGDANOV, JONATHAN E. GRINDLAY, AND GEORGE B. RYBICKI
sbogdanov@cfa.harvard.edu, josh@cfa.harvard.edu, grybicki@cfa.harvard.edu
Harvard-Smithsonian Center for Astrophysics, 60 Garden Street, Cambridge, MA 02138
Draft version September 29, 2018

ABSTRACT

X-ray emission from many rotation-powered millisecond pulsars (MSPs) is observed to be of predominantly thermal nature. In PSR J0437–4715, the nearest MSP known, an additional faint power-law tail is observed above 2.5 keV, commonly attributed to non-thermal magnetospheric radiation. We propose that the hard emission in this and other similar MSPs is instead due to weak Comptonization of the thermal (blackbody or hydrogen atmosphere) polar cap emission by energetic electrons/positrons of small optical depth in the pulsar magnetosphere. This spectral model implies that all soft X-rays are of purely thermal origin, which has profound implications in the study of neutron star structure and fundamental pulsar physics.

Subject headings: pulsars: general — pulsars: individual (PSR J0437–4715) — stars: neutron — X-rays: stars

1. INTRODUCTION

As the nearest and brightest rotation-powered millisecond pulsar (MSP), PSR J0437–4715 (Johnston et al. 1993; van Straten et al. 2001) has been the best studied in the X-ray domain. *ROSAT*, *Chandra*, and *XMM-Newton* observations (Zavlin & Pavlov 1998; Zavlin et al. 2002; Zavlin 2006) have revealed that the emission in the 0.1–10 keV band consists of two thermal components, and a faint power-law (PL) tail, with photon index $\Gamma \sim 2$. The latter can only be discerned in the spectrum beyond 2.5 keV. Due to the limited spectral information above ~ 3 keV, the nature of this hard X-ray component is unclear.

In this *Letter*, we examine the plausibility of various emission mechanisms capable of producing the hard X-rays observed from J0437–4715 (henceforth J0437). The paper is organized as follows. In §2 we describe the observations used and their analysis while §3 outlines various interpretations of the emission from J0437. In §4 we present the results of our analysis and offer a discussion and conclusions in §5.

2. OBSERVATIONS AND DATA REDUCTION

We have retrieved archival *Chandra* and *XMM-Newton* observations of J0437 to investigate the X-ray emission from this MSP. The *Chandra* ACIS-S observations were performed on 2000 May 29–30 (25.7 ks effective exposure, 3.9' off axis; see Zavlin et al. 2002, for details). We first reprocessed the level 1 event files using the most recent calibration release and the CIAO 3.3 software package¹. The data were then filtered to the nominal *Chandra* energy band (0.3–8 keV). The source counts were obtained from a 5" circular region centered on the radio position of the MSP. This circle encloses $>90\%$ of the total energy.

The *XMM-Newton* data consist of a 70-ks observation with the EPIC-MOS1/2 detectors in full-frame mode and EPIC-pn instrument in fast timing mode obtained on 2002 October 9 (see Zavlin 2006). The raw data were reprocessed using the `emchain` and `epchain` pipelines of

the SAS 6.5.0 software² and were screened for instances of high background flares, which were subsequently removed. In the case of MOS1/2, the source counts were extracted from 70" circles, which enclose $>90\%$ of the total energy. To minimize background contamination the MOS1/2 data were restricted to the 0.3–8 keV band. For the pn detector, the MSP counts were extracted from CCD columns 28–39 and were filtered to 0.5–10 keV, where the detector response is best known.

For all observations, the background was obtained from a source-free region near the position of the MSP. The spectral fits were performed in XSPEC 11.3.1³.

3. ORIGIN OF THE HARD X-RAY TAIL

The inherent faintness of the hard PL component from J0437 and the limited bandwidth over which it can be observed pose an obstacle in deciphering the origin of this emission. Nonetheless, using the available data we can by gain more insight by examining the plausibility of the various mechanisms for production of the observed hard X-ray tail.

3.1. *Non-thermal Emission*

The most widely accepted model for production of a PL spectrum in pulsars involves non-thermal radiation by relativistic electrons and positrons (e^\pm) in the pulsar magnetosphere. The analyses by Zavlin et al. (2002) and Zavlin (2006) of *Chandra* and *XMM-Newton* observations found that the hard X-ray tail seen in J0437 is well described by a PL with spectral index $\Gamma = 2.0 \pm 0.4$. Under the assumption that this emission is of non-thermal magnetospheric origin, the PL is expected to extend from the optical/UV and beyond the hard X-ray range (>10 keV). However, *Hubble Space Telescope* FUV observations have revealed that extrapolation of the powerlaw to lower energies is inconsistent with the FUV flux from the MSP, with the lower bound $\Gamma \approx 1.6$ only marginally consistent with the FUV flux (Kargaltsev et al. 2004).

² Science Analysis Software, available at <http://xmm.vilspa.esa.es/>

³ <http://heasarc.gsfc.nasa.gov/docs/xanadu/xspec/>

¹ Chandra Interactive Analysis of Observations, available at <http://asc.harvard.edu/ciao/>

The measured FUV flux is otherwise consistent with that of $\sim 10^5$ K thermal emission from the whole NS surface. The apparent discrepancy casts doubt on the validity of the PL model.

Becker & Trümper (1999) have proposed that the X-ray emission from J0437 and other nearby MSPs (e.g. PSRs J0030+0451 and J2124–3358) could be due to non-thermal processes in the magnetosphere. However, based on more recent observations of these MSPs, we conclude that this interpretation is untenable. If the emission were indeed of purely non-thermal character, then such a broken PL spectrum grossly overestimates the observed optical/UV fluxes (Koptsevich et al. 2003; Mignani & Becker 2003; Kargaltsev et al. 2004) unless yet another break exist below 0.1 keV. No such behavior is observed in the X-ray spectra of other pulsars, in particular the luminous MSPs B1937+12 and B1821-24, which show purely non-thermal pulsed radiation (see e.g., Becker et al. 2003; Mineo et al. 2004).

An alternative source of non-thermal X-rays is nebular synchrotron emission from an intrabinary shock formed due to interaction between the wind from the MSP and the companion star. Such a shock is believed to be present in other binary MSPs, namely PSRs B1957+20 (Stappers et al. 2003), J0024–7204W (Bogdanov et al. 2005), and J1740–5340 (Grindlay et al. in preparation). However, for J0437, the strength of the pulsar wind $\dot{E} \sim 4 \times 10^{33}$ ergs s^{-1} and the orbital separation⁴ of $a = 1.2 \times 10^{12}$ cm do not favor this interpretation as the expected X-ray luminosity from the resulting shock is substantially lower than observed. Specifically, assuming a radius $\sim 1.5 \times 10^9$ cm for the $0.24 M_{\odot}$ white dwarf (WD) companion (van Straten et al. 2001), we find that the total incident power on the face of the WD from the pulsar wind is $\sim 10^{27}$ ergs s^{-1} , more than two orders of magnitude lower than the observed luminosity of the hard emission ($L_X \approx 7 \times 10^{29}$ ergs s^{-1} for 0.1–7 keV). The large discrepancy can be reduced in a more contrived scenario, involving a highly anisotropic wind, confined to the orbital plane in a beam covering $< 0.15\%$ of the sky. Alternatively, the companion may be bloated or surrounded by a large tenuous envelope of gas that interacts with the MSP wind. However, this assertion is in conflict with the observed optical properties of J0437, which are entirely consistent with that of a $\sim 0.2 M_{\odot}$ He-WD (see e.g., Bailyn 1993). Therefore, we conclude that an intrabinary shock is not a significant source of X-ray emission in the J0437 system.

3.2. Thermal Emission

In a purely thermal scenario the hard emission from J0437 may originate from a very small hot spot on the polar cap with a radius of order a few meters, radiating at temperatures in excess of 8×10^6 K. However, no current MSP polar cap heating model predicts such peculiarly high temperatures and small emission areas, making this model rather implausible. The validity of this model can be tested by deep observations at $\gtrsim 3$ keV.

3.3. Comptonized Thermal Emission

⁴ In Zavlin et al. (2002) the semi-major axis of the MSP (a_1) is erroneously quoted as being the distance between the MSP and its companion ($a = a_1 + a_2$).

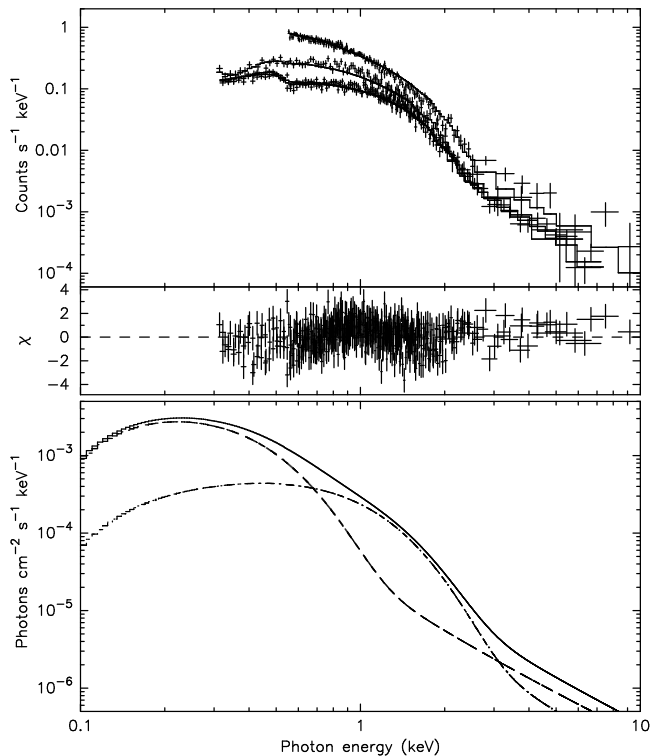


FIG. 1.— (top) *Chandra* ACIS-S and *XMM-Newton* EPIC-MOS1/2 and EPIC-pn spectra of J0437 fitted with a two temperature Comptonized blackbody model (*compbb*). The lower panel shows the best fit residuals. (bottom) Model spectra used in the fit. The solid line is the total spectrum, while the dashed and dot-dashed lines show the individual emission components (see text for best fit parameters).

The hard X-ray tail can be naturally produced by re-processing of the thermal emission via inverse Compton scattering (ICS) by an optically thin ($\tau < 1$) hot plasma. As a thermal photon emitted at the NS surface propagates through the tenuous co-rotating plasma in the pulsar magnetosphere, it may undergo ICS by energetic e^{\pm} . In this regime, repeated scatterings of the thermal seed photons result in a PL distribution of photons (see Rybicki & Lightman 1979; Nishimura et al. 1986). Due to the low τ of the magnetospheric plasma, only a small fraction of the thermal photons are scattered, resulting in a faint Comptonized tail.

A major advantage of this model is that, unlike the case of a non-thermal (magnetospheric) PL, it does not extend below ~ 1 keV (see Fig. 1), thus, alleviating any discrepancies with optical/UV data. Therefore, based on the available observational evidence and the relative simplicity of the Comptonization model, we deem this interpretation the most plausible.

4. RESULTS

We have examined the effect of inverse Compton scattering (ICS) on the thermal emission from MSPs for both a blackbody (BB) and neutron star hydrogen atmosphere (NSA, see Romani 1987; Zavlin et al. 1996) model. For the BB case we employed the *compbb* model in XSPEC (Nishimura et al. 1986). This particular model assumes a plane-parallel, semi-infinite scattering medium with the

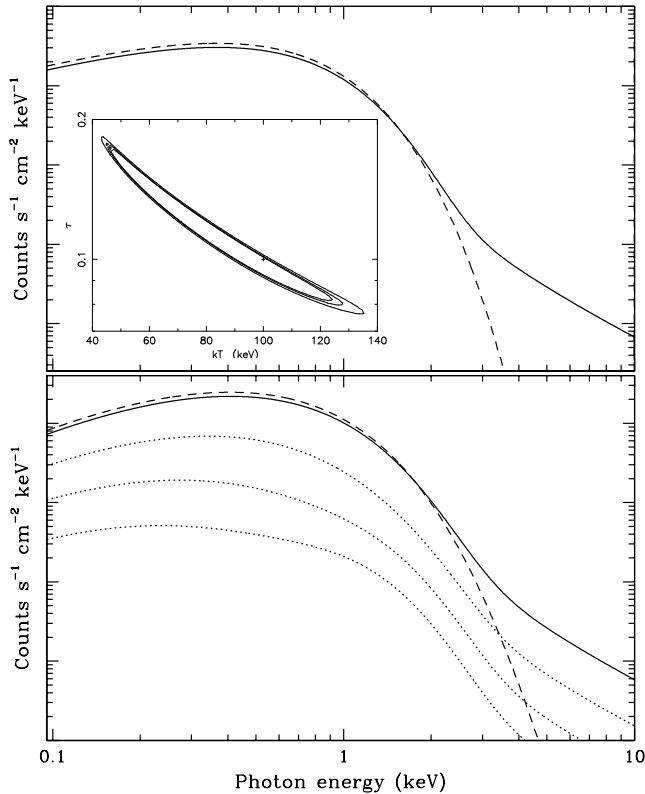


FIG. 2.— (*top*) Example Comptonized BB model spectrum for $kT_{\text{eff}} = 0.23$ keV, $kT_e = 100$ keV, and $\tau = 0.1$. The dashed line shows the initial thermal photon distribution. The inset shows example 1-, 2-, and 3 σ contours for τ versus kT_e to illustrate the correlation between the two parameters. (*bottom*) Comptonized NSA model (Heinke et al. 2006) spectrum for $T_{\text{eff}} = 1.3 \times 10^6$ K, $kT_e = 100$ keV, and $\tau = 0.1$. The photon energies have been corrected for the gravitational redshift assuming $R = 10$ km and $M = 1.4 M_{\odot}$. The dotted lines correspond to different viewing angles relative to the surface normal ($\cos \theta = 0.5, 0.25,$ and 0.1 , from top to bottom, respectively), while the solid line is for $\cos \theta = 1$. In both plots the dashed line shows the initial thermal photon distribution. The flux normalization is arbitrary.

source of thermal photons at the bottom. It is valid over the range $E \ll kT_e < mc^2$, where E is the initial photon energy, T_e is the scattering e^{\pm} temperature, and mc^2 is the electron rest energy. Figure 1 shows the X-ray spectrum of J0437 fitted with a two-temperature Comptonized BB model using `compbb`. Throughout the spectral fits we fixed the hydrogen column density towards the MSP to $N_{\text{H}} = 2 \times 10^{19} \text{ cm}^{-2}$ and electron temperature to $T_e = 150$ keV. The best fit parameters we obtain are $T_1 = (2.93 \pm 0.03) \times 10^6$ K, $R_1 = 44 \pm 11$ m, $\tau_1 = 0.06 \pm 0.02$, $T_2 = (1.16 \pm 0.01) \times 10^6$ K, $R_2 = 300 \pm 40$ m, and $\tau_2 = 0.09 \pm 0.01$. The corresponding luminosity in the 0.3–10 keV is found to be $L_X \approx 3 \times 10^{30} \text{ ergs s}^{-1}$. All uncertainties quoted above are 1σ . The minimum value of $\chi^2_{\nu} = 1.36$ (for 464 degrees of freedom) was found to be identical to that in the case of the BB+BB+PL model. Given the uncertainties in the cross-calibration of the different detectors, this value of χ^2_{ν} indicates an acceptable fit. As is generally the case for ICS, T_e and τ are strongly correlated (see inset in Fig. 2) so a good fit was obtained for a wide range of kT_e and τ .

The `compbb` model assumes a thermal distribution of scattering e^{\pm} . In reality, these particles probably follow a non-thermal (PL) distribution over a certain range of energies. Notwithstanding, the exact energy distribution of the e^{\pm} has no bearing on the validity of this model since in both cases, multiple scatterings result in a PL distribution of photons.

To study the effect of Comptonization on the emission from a NSA we used the unmagnetized hydrogen atmosphere model from Heinke et al. (2006) (see also McClintock et al. 2004) and the Comptonization algorithm of Nishimura et al. (1986). As expected, we have found that the NSA model yields a qualitatively similar spectrum to that of the BB case (see Fig. 2). However, crucial differences do exist, stemming from the inherently anisotropic and energy dependent emission pattern of a NSA (Zavlin et al. 1996). In particular, at a given viewing angle, the intensity of the NSA radiation is subject to limb darkening as well as a projection effect. The scattered photons, on the other hand, probably have a different angular distribution. This suggests that depending on the viewing geometry, the observed flux may show variations in the relative contribution from the Comptonized component.

It is important to emphasize that the exact geometry and location of the scattering medium relative to the MSP polar caps is unknown and cannot be determined from the time integrated spectra alone. In principle, these properties can be inferred by studying the modulation of the Comptonized radiation as a function of the rotational phase of the MSP. To investigate the temporal behavior of the PL tail, we used the timing data from the *XMM-Newton* EPIC-pn detector. Figure 3 shows lightcurves of J0437 folded at the MSP spin period ($P = 5.76$ ms) for the 0.3–1 keV and 3–6 keV energy ranges. In the Comptonization scenario, these two bands contain purely (unscattered) thermal and just Comptonized photons, respectively. Unfortunately, due to the limited count statistics and the high instrument and sky backgrounds, which dominate the emission for >3 keV, at present, we cannot provide any meaningful constraints on the properties of the Comptonizing medium. We are, however, able to place a limit on the pulsed fraction of $\lesssim 50\%$ for >3 keV. This value further constrains a non-thermal magnetospheric origin since such emission is expected to be almost entirely pulsed.

5. DISCUSSION AND CONCLUSION

We have demonstrated that the X-ray emission from the nearby MSP J0437 in the 0.1–10 keV band is well described by a two-temperature Comptonized thermal spectrum. This model provides an attractive and relatively simple alternative to the non-thermal magnetospheric emission model. Since in the Harding & Muslimov (2002) model of high-energy emission from MSPs, ICS is the primary mechanism for pair production and polar cap heating, the presence of a hard Comptonized tail would provide a strong confirmation that this mechanism does indeed operate in MSP magnetospheres.

We note that the shape of the spectra in the non-thermal magnetospheric and Comptonization cases are indistinguishable in the 0.1–10 keV band. The primary difference arises in the optical/UV range, where only

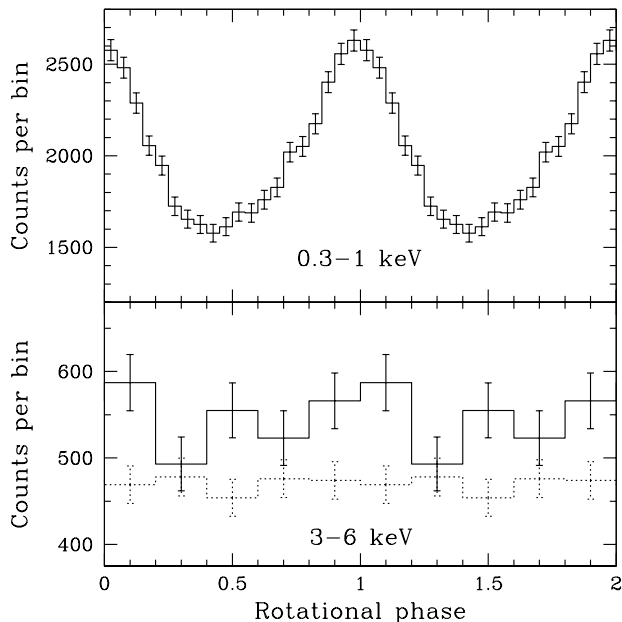


FIG. 3.— *XMM-Newton* EPIC-pn lightcurves of J0437 in the 0.3–1 keV (*top*) and 3–6 keV (*bottom*) bands. The dotted line in the bottom panel shows the background level. Two cycles are shown for clarity.

the former is expected. As mentioned previously, for J0437 the non-thermal model has been found to be only marginally consistent with FUV observations. The detection of a hard X-ray tail from other near-by MSPs such

as PSRs J0030+0451 and J2124–3358, would provide a more definitive test of the two interpretations (the existence of a hard X-ray component cannot be ascertained in present X-ray observations of these MSPs due to the limited counts). For these solitary MSPs, the absence of a stellar companion has allowed ultra-deep optical observations, which have found no emission down to $V \sim 28$ (Koptsevich et al. 2003; Mignani & Becker 2003).

The Comptonization model proposed in this *Letter* implies that *all* of the soft emission (<1 keV) from J0437–4715 is purely thermal (unscattered) radiation. This has profound ramifications in the study of fundamental NS properties since thermal emission from the surface of neutron stars reveals important information regarding the basic properties of this class of compact objects. Pavlov & Zavlin (1997) have shown that X-ray spectral and timing observations of MSPs can be used to measure fundamental NS parameters such as the mass-to-radius ratio (M/R) of the underlying NS. In addition, the polar caps represent “footprints” of the pulsar magnetic field, allowing constraints on the global field geometry. Finally, since the properties of the hard emission component are determined by the energy distribution of scattering particles and their optical depth, study of this radiation can also serve as a probe of the particles populating the pulsar magnetosphere. An attempt to constrain the properties of J0437 outlined above is currently under way and will be presented in a future paper.

This work was supported in part by NASA grant AR6-7010X. The research presented here has made use of the NASA Astrophysics Data System (ADS).

REFERENCES

- Bailyn, C. D. 1993, *ApJ*, 411, L83
 Becker, W. & Trümper, J. 1993, *Nature*, 365, 528
 Becker, W. & Trümper, J. 1999, *ApJ*, 341, 803
 Becker, W. & Aschenbach, B. 2002, *Proceedings of the 270. WE-Heraeus Seminar on Neutron Stars, Pulsars, and Supernova Remnants*, Eds. W. Becker, H. Lech, J. Trümper, p. 64
 Becker, W., Swartz, D. A., Pavlov, G. G., Elsner, R. F., Grindlay, J., Mignani, R., Tennant, A. F., Backer, D., Pulone, L., Testa, V., & Weisskopf, M. C. 2003, *ApJ*, 594, 798
 Bogdanov, S., Grindlay, J. E., & van den Berg, M. 2005, *ApJ*, 630, 1029
 Bogdanov, S., Grindlay, J. E., Heinke, C. O., Camilo, F., Freire, P. C. C., & Becker, W. 2006, *ApJ*, in press
 Harding, A. K. & Muslimov, A. G. 2002, *ApJ*, 568, 862
 Heinke, C. O., Rybicki, G. B., Narayan, R., Grindlay, J. E. 2006, *ApJ*, in press, astro-ph/0506563
 Johnston, S., Lorimer, D. R., Harrison, P. A., Bailes, M., Lyne, A. G., Bell, J. F., Kaspi, V. M., Manchester, R. N., D’Amico, N., & Nicastro, L. 1993, *Nature*, 361, 613
 Kargaltsev, O. Y., Pavlov, G. G., & Romani, R. W. 2004, *ApJ*, 602, 327
 Koptsevich, A. B., Lundqvist, P., Serafimovich, N. I., Shibanov, Yu. A., & Sollerman, J. 2003, *A&A*, 400, 265
 McClintock, J. E., Narayan, R., & Rybicki, G. B. 2004, *ApJ*, 615, 402
 Mignani, R. P. & Becker, W. 2003, *AdSpR*, 33, 616
 Mineo, T., Cusumano, G., Massaro, E., Becker, W., & Nicastro, L. 2004, *A&A*, 423, 1045
 Nishimura, J., Mitsuda, K., & Itoh, M. 1986, *PASJ*, 38, 819
 Pavlov, G. G. & Zavlin, V. E. 1997, *ApJ*, 490, L91
 Romani, R. W. 1987, *ApJ*, 313, 718
 Rybicki, G. B. & Lightman, A. P. 1979, *Radiative Processes in Astrophysics* (New York: Wiley)
 Stappers, B. W., Gaensler, B. M., Kaspi, V. M., van der Klis, M., & Lewin, W. H. G. 2003, *Science*, 299, 1372
 van Straten, W., Bailes, M., Britton, M., Kulkarni, S. R., Anderson, S. B., Manchester, R. N., & Sarkissian, J. 2001, *Nature*, 412, 158
 Zavlin, V. E., Pavlov, G. G., & Shibanov, Yu. A. 1996, *A&A*, 315, 141
 Zavlin, V. E. & Pavlov, G. G. 1998, *A&A*, 329, 583
 Zavlin, V. E., Pavlov, G. G., Sanwal, D., Manchester, R. N., Trümper, J., Halpern, J. P., & Becker, W. 2002, *ApJ*, 569, 894
 Zavlin, V. E. 2006, *ApJ*, 638, 951
 Zhang, L. & Cheng, K. S. 2003, *A&A*, 398, 639